Severity Assessment of Social Anxiety Disorder in Default Mode Network using EEG signals

Abdulhakim Al-Ezzi[a], Nidal Kamel[a]*, and Esther Gunaseli[b]

[a]*Centre for Intelligent Signal and Imaging Research (CISIR) Department of Electrical and Electronic Engineering, Universiti Teknologi PETRONAS, Malaysia*

[b]*Universiti Kuala Lumpur, Psychiatry Discipline Sub Unit, Perak, Malaysia*

Abstract

Brain neuroimaging studies have found that social anxiety disorder (SAD) is correlated with aberration in regional or network-level brain function. In this study, SAD-related alternation in brain connections within the default mode network (DMN) was investigated. Partial directed coherence (PDC) was used to assess the causal influences of DMN regions on each other and indicate the changes in the DMN effective network related to SAD severity. Electroencephalogram (EEG) data were collected from 89 subjects (control, mild, moderate, severe), and a causal network between eight fundamental regions belonging to the DMN was established. Among the healthy control (HC) and the three considered levels of severity of SAD, the results indicated a higher level of causal interactions for the mild and moderate SAD groups than for the severe and HC groups. Between the control and the severe SAD groups, the results indicated a higher level of causal connections for the control throughout all the DMN regions. We found significant increases in the mean PDC in the delta and alpha bands between the SAD groups. Among the DMN regions, the precuneus exhibited a higher level of causal influence than other regions. Therefore, it was suggested to be a major source hub that contributes to the mental exploration and emotional content of SAD. In contrast to the severe group, the HC exhibited a higher resting-state connectivity at the mPFC, providing evidence for mPFC dysfunction in the severe SAD group. Furthermore, the total Social Interaction Anxiety Scale (SIAS) scores were positively correlated with the mean values of the PDC of the severe SAD group and negatively correlated with those of the HC group. This study reveals the network measures for several SAD groups in the DMN at different frequency bands. The reported results may facilitate greater comprehension of the underlying potential SAD neural biomarkers and can be used to characterize possible targets for further medication.

Keywords: Effective connectivity network, Granger causality (GC), Social Anxiety Disorder (SAD), Default Mode Network (DMN), Electrophysiological biomarkers (EEG), Partial directed coherence (PDC).

ARTICLE INFO		* *Corresponding author.*
RECEIVED	March 16, 2021	Email: *nidalkamel2@hotmail.com*
REVIEWED	June 14, 2021	
ACCEPTED	August 18, 2021	

1. Introduction

Social anxiety disorder (SAD), sometimes referred to as social phobia, is one of the most negative common mental disorders caused by an overwhelming fear of negative evaluation by others in social situations. SAD is an intense persistent fear with a current lifetime prevalence between 8.4 and 15 %. SAD is associated with a general trepidation and avoidance of social situations (Stein et al., 2008). It is believed to be correlated with additional negative conditions and behaviors, such as abuse and destructive use of substances, insomnia disorder, depression, mood disorder, and even suicidal behavior (Kessler et al., 1999), (Koyuncu et al., 2019), (Lemyre et al., 2019). Generally, SAD is found to extremely affect both the physical and psychological behaviors of individuals (Von Dawans et al., 2018). Thus, SAD recognition is a crucial element in different domains such as characterizing the level of individuals' mental and physical states, recognizing the level of anxiety, quantifying stress in social situations.

To strengthen research in SAD recognition and provide effective therapy for individuals with SAD, researchers and clinicians attempted to have effective evaluation instruments for characterizing the disorder in terms of its diagnostic basis. Different biomarkers including heart rate (HR) and electrocardiogram (ECG), physiological alterations between sequential heartbeats, electrodermal response, and neuro-electrophysiological signals have been used to assess the severity of SAD (Pittig et al., 2018). There are many functional brain imaging mechanisms developed to evaluate the brain functions that can be used to acquire substantial information related to brain activity of patients with SAD. Among these techniques, electroencephalogram signals (EEG) is the most common mechanism of estimating electric fields potentials generated by various neural activities of the brain. Furthermore, the EEG can be captured noninvasively, with portable EEG machine and cost-effective than other neuroimaging techniques that are utilized in SAD diagnosis. The neural cells transmit information to each other by electrical impulses (cells communication) (Hoehn Saric, 1982). These neuroelectrical impulses generated inside the brain can be captured and recorded by the metal electrodes mounted on the scalp with the assistance of EEG amplifiers. The EEG measures make it feasible to extract significant information about different emotional states (e.g., anxiety, depression). Recent research in neuroscience has proven that SAD affects the neural activities within the human brain (Wolpaw et al., 2002), (Brigham et al., 2010). SAD is correlated with a perturbation in the neural communication system involved in emotional self-regulation, perceptual stimulus distortion, and emotional stability characteristics. An extensive review of the major frequently deliberated EEG biomarkers related to SAD is summarized in this recent article (Al-Ezzi et al., 2020).

2. Default Mode Network

In neuroscience, the default mode network (DMN) is a large-scale brain network essentially made of the mesial prefrontal cortex (mPFC), posterior cingulate cortex (PCC)/precuneus, and lateral partial cortex (angular and supramarginal gyrus) (Tao et al., 2015). It is best recognized for being active when a person is not concentrated on the external world and the brain is at vigilant rest, such as during self-referential and mind-wandering (Lin et al., 2017). Additionally, the DMN is also can be found to be active when a person thinks about themselves, about others, retrieval of memory, and future planning (Sheline et al., 2017). On the other hand, the DMN was primarily found to be deactivated in goal-oriented tasks (e.g., physical activities, attentional tasks, and arithmetic tasks) . Neuroscience suggests that the DMN is able to contribute to the neuropsychological investigation of cognitive and social functionality, which can assist in delineating the neural biomarkers of SAD (Qiu et al., 2011). The DMN network has been involved in cognitive processes and many different brain activities such as spatial cognition, social cognition, attention, and motor intent, and higher cognitive functions.

DMN impairment is found to be involved in some mental pathology conditions, including autism (Spencer et al., 2012) and depression (Sheline et al., 2017). Moreover, this dysfunction can serve as the foundation of self-information regulation and emotional process bias in the SAD (Ding J. et al., 2011). The resting-state functional connectivity (FC) features in the DMN of SAD patients and HCs were compared and the findings revealed that the FC between different cortical regions in the aged people was greater than in the youths (Chen et al., 2013). Furthermore, the influence of SAD on the prefrontal brain was estimated using structural and functional MRI studies (Andreescu et al., 2014). Specifically, in HCs and SAD individuals, a variance was observed in the resting-state FC between the hippocampus and the limbic-prefrontal circuit in the DMN network (Chen et al., 2013). The DMN has revealed greater connectome in the resting state when an individual was more focused internally rather than externally or on attention-demanding tasks (Tao et al., 2015). However, up till this, no specific study has investigated the severity assessment of SAD using effective connectivity in DMN network.

3. Effective connectivity

Effective connectivity (EC) is defined as the influence that a set of neurons exerts over another under a network model of causal dynamics and is inferred from a model of neuronal integration, which defines the mechanisms of neuronal coupling (Valdes-Sosa et al., 2011). Brain connectivity is established when neurons of one brain region are coupled with neurons of other brain regions and associate dynamically by regulating their rhythms with each other. Recently, there has been growing interest among researchers in studying both normal and pathological brain functions not only through variations in activation between brain areas, but also via interactions among the neural assemblies dispersed over different brain regions (Beaty et al., 2019). This network of interactions between various regions of the brain is called brain connectivity (Busby et al., 2019). Brain connectivity can be explained in terms of structural, functional, and effective connectivity. Fibre pathways physically extend from one brain region to another, representing structural connectivity (Sokolov et al., 2019). These fiber tracts can be best observed using MRI and diffusion tensor imaging (DTI) technique (Richards et al., 2015). Apart from being structurally connected, brain regions may become functionally connected, i.e., the neuronal activities among different brain regions become statistically dependent while performing a function. This type of

statistical dependence is commonly referred to as functional connectivity (FC) (Greicius et al., 2009). To avoid the fundamental drawbacks of FC, in terms of its bidirectional nature and susceptibility to connection with a third party, a relatively new concept called effective connectivity (EC), was proposed (Valdes-Sosa et al., 2011). EC reflects the causal interaction between the driver (initiating external force) and the response (the driven system); it has a more direct influence on one neural system of a brain region than over others and defines dynamic directional interaction among them (Valdes-Sosa et al., 2011). This influence can be directly estimated through signals and called data-driven EC or is named based on a model that specifies causal links among different brain regions, termed model-driven EC (Bakhshayesh et al., 2019). An fMRI-based resting state study (Liao W. et al., 2010) was the first study to reveal and quantify an abnormal brain network via the assessment of EC in individuals with SAD. The effect of the ventral cerebral cortex on the amygdala was found to be reduced in the SAD group significantly more than in the HC group, while the causal effect between the limbic system (amygdalan components) and the visual cortex was increased using GC analysis. In a previous study (Sladky et al., 2013), SAD patients showed a positive correlation between the frontal cortex and the amygdala, which indicates the presence of excitatory connectivity. An abnormal amygdala is often found in patients with SAD (Engel et al., 2001), (Freitas-Ferrari et al., 2010) based on EC.

4. Materials and methods

4.1. Participants

We recruited 88 subjects from 502 respondents who recorded their self-assessment of the SIAS and were aged between 18–24 years, 36 females (mean (M) =21.97, standard deviation (SD) = 0.98), and 53 males (M=22.73, SD=0.84). The diagnostic procedure was on the basis of the Structured Clinical Interview for DSM-IV (Ventura et al., 1998) and the clinical administered Social Interaction Anxiety Scale (SIAS; (Liebowitz et al., 1985) determined the severity of SAD. Accordingly, the participants were assigned to four different categories: control (SAIS score < 20), mild (SIAS score < 35), moderate (SIAS score < 50), and severe (SIAS score ≥ 50). None of the participants had any history of psychotropic medications, neurological, or surgical disabilities, which may impair brain function or metabolic functions. Participants with major mental illness (e.g., bipolar, psychotic, and other disorders) were excluded.

4.2. Experimental design

The resting-state (RS) recordings were conducted completely at the EEG laboratory. Participants were instructed to be seated comfortably, let their minds wander freely with their eyes closed, in a quiet, mid-dark room; EEG-RS data were recorded for approximately 4–6 min. Real-time EEG data were consistently recorded in RSN using a referential 32-channel shielded cap (ANT Neuro, Enschede, Netherlands). The electrodes were mounted according to the international standard 10–20 system with impedances maintained below 10 kΩ. Moreover, the procedure for this study has been closely reviewed, endorsed, and approved by the Medical Science Ethics Committee of the Royal College of Medicine of Perak, Kuala Lumpur University

4.3. EEG Acquisition and EEG data processing

The electrophysiological information was recorded at a sampling rate of 2048 Hz and was later downsampled to 256 Hz. The original EEG dataset was then pre-processed offline to eliminate unnecessary data (noised segments) by using BESA research toolbox 6.0. To eliminate the high-frequency electrocortical artifacts, signal noise, and low-frequency deflections, we applied a band-pass filter to acquire the superlative segments between the frequency range of 0.4 and 50 Hz. Artifacts such as eye blinks, eye motions, breathing, power interference, and cardiac movements were visually inspected and discarded. We have also applied spatial filters based on artifact detection and correction and brain signal topographies provided by BESA [59]. Moreover, we used the following open-source toolboxes: EEGLAB for topographic map visualization (Delorme et al., 2004). To compute the directed causal coherence (i.e., PDC) among channel pairs, RS data was segmented into 3-second trials (a total of 180 s), which is in the range of other RS studies (Yu M. et al., 2016), (Fraga González et al., 2016). Each subject's data was calculated to find the average values for all segments. Specifically, the averaged spectral effective connectivity was computed separately for every channel considering the following frequency bands: delta (1–3 Hz), theta (4–8 Hz), alpha (9–12 Hz), and beta (13–30 Hz). The whole process of our study is shown in Fig.1.

4.4. Partial directed coherence (PDC)

The conception of PDC was proposed by Baccala and Sameshima in 2001 (Baccalá et al., 2001), put forward a new frequency-domain method for the description of Granger Causality (GC). However, the PDC provides another estimation technique for the association between a pair of neuronal signals, which defines the correlation between regions i and j. The PDC from channel j to channel i indicates the directional flow of information from one activity site in to another. As mentioned earlier, these PDC values are in the range of [0, 1] (Baccalá et al., 2001). Compared with the functional connectivity computed using the coherence algorithms, the effective connection computed by the PDC is a directional value representing the causal interaction, i.e., the influence of one neuron system over another. Moreover, the PDC has the ability to identify the indirect and direct connections between processes by removing the impacts of all other channels in the system (Blinowska, 2011).

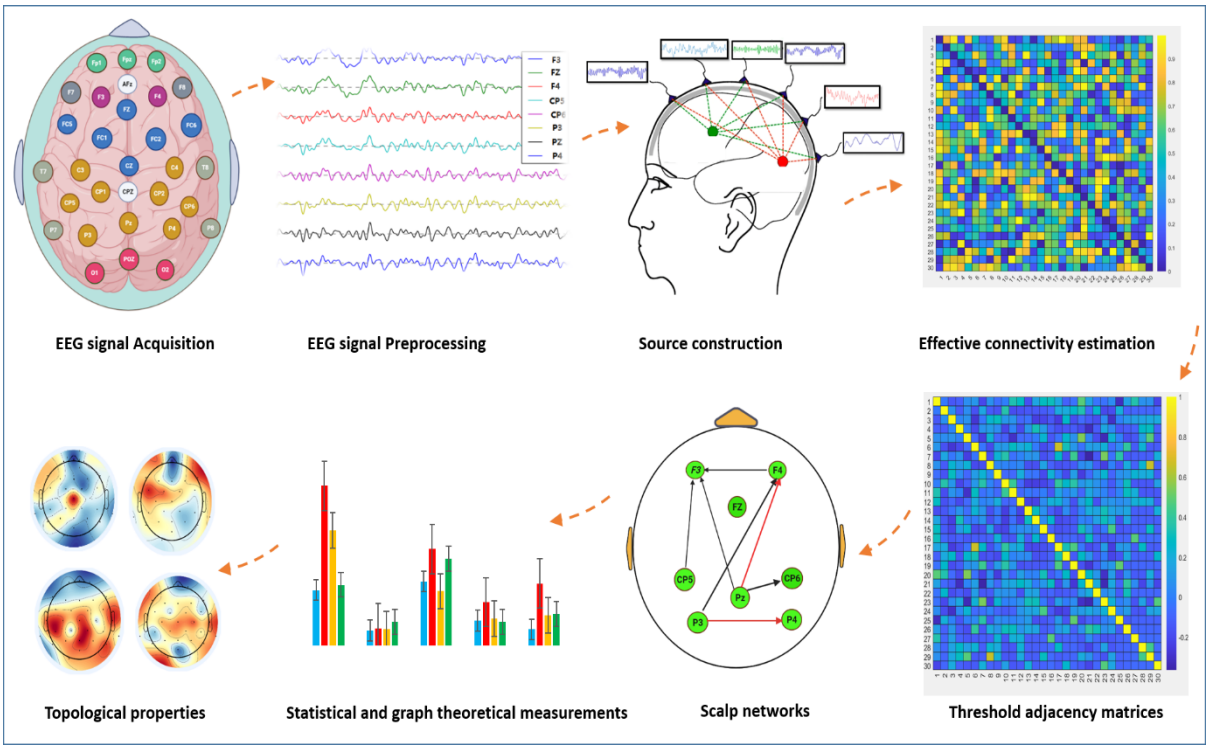

Fig.1. Block diagram for the EEG data analysis module to identify the parameters of the EC network based on the EC.

Generally, an MVAR model with a number of cortical DMN regions (m electrodes) of EEG signals and order p is defined as follows:

$$X(t) = \sum_{r=1}^{p} A\,(r)\,X\,(t-r) + E(t), \quad (1)$$

where

$$Al = \begin{bmatrix} a_1(l) & \cdots & a_{1n}(l) \\ \vdots & \ldots & \vdots \\ a_n(l) & \ldots & a_{nn}(l) \end{bmatrix}, \quad (2)$$

is the coefficient matrix at the time lag (l).

where, X (t) represents the weight vector of m electrodes of EEG signals at time t, matrix A (r) indicates the r^{th} order AR parameters, and E (t) represents the measured error that is believed to be an independent Gaussian process with zero mean. When the coefficients of the MVAR model are adequately calculated, A (F) is determined as follows:

$$A(F) = \sum_{r=1}^{p} A(r)e^{-i2\pi fr}, \quad (3)$$

Therefore, the PDC value from channel j to channel i can be expressed as follows:

$$PDC_{ij}\,(f) = \frac{A_{ij}\,(f)^{-}}{\sqrt{aj^{-H}\,(f)aj^{-}(f)}}, \quad (4)$$

where, āi (f) (i = 1, 2, …M) represents the i^{th} column of the matrix Ā(f) and PDCij represents the directional influence and intensity of the information flow from channel j to channel i at a frequency of f.

4.5. EEG source localization

The acquired EEG signals can be used to perform the inverse problem to define the exact locations and current distribution of the predominant sources of the neurons that are synchronously and simultaneously active. To provide more validity to this approach, an additional source localization analysis of all frequency oscillations (0.4–50Hz) in RS was performed using exact low-

resolution brain electromagnetic tomography (eLORETA) in search of the active sources generating the scalp potentials (Pascual-Marqui et al., 2011). The eLORETA mechanism is a discrete, three-dimensional (3D) distributed, linear, weighted minimum norm inverse solution and has the ability to reconstruct intercortical activity with correct localization from scalp EEG data (Grech R. et al., 2008), (Lopez Rincon et al., 2016). The source model of eLORETA and the cerebral region coordinates are established based on the Montreal Neurological Institute average MRI brain map (MNI) with 15000 vertices of the cortex surface as reported in (Imperatori et al., 2014). The algorithm of eLORETA is explained in detail in (Pascual-Marqui, 1985). We have excluded the non-active cortical areas from further EC analysis. Eight (8) electrodes were found to be active among all subjects (e.g., F3, F4, Fz, CP5, CP6, P3, P4, and Pz). Directed connectivity weights between these active regions were calculated for each artifact-free EEG segment in the following frequency bands: delta (1–3 Hz), theta (4–8 Hz), alpha (9–12 Hz), low beta (13-21) and high beta (22–30 Hz).

4.6. Power analysis and EEG frequency decomposition

The constructed EEG signals and all epoch's parameters are coordinated with PDC and Fast-Fourier transforms. All subject's data were segmented and averaged across all EEG channels and the mean absolute power measures were computed for each of the following frequency bands: Delta (0.5–4 Hz), Theta (4–8 Hz), Alpha (8–12 Hz), Beta (13–30 Hz). A 50% overlapping Hanning window was applied to minimize spectral leakage.

4.7. Statistical analysis

All the statistical findings were presented as the mean ± SD. The analysis of mean variances in our study included two independent variables and one dependent variable (Group: severe, average, mild and controlled) * (Regions; F3, F4, P3, P4 ...) * (DMN EC values)); therefore, a one-way bivariate ANOVA and Tukey's HSD post-hoc test for various comparisons ($p < 0.05$) were performed to assess the main significant differences between SAD groups. To assess the effect of the region on the EC data, an ANOVA test ($p < 0.05$) was performed to identify the significant differences between the DMN regions and EC measures. Additionally, the Pearson correlation coefficients between the SIAS scores and the mean EC in the resting-state DMN were calculated separately for each group (control, moderate, medium, and severe). After computing these spectral EC values, we examined how the EC values varied among SAD groups. SPSS (version 25.0.0.0, IBM Corp., Armonk, NY) was used for all the statistical analyses.

5. Result and discussion

5.1. Subjective data analysis

Initially, we examined the self-assessment reports data to determine the group differences in different frequency bands. The total calculated percentages of the SAD groups—control, mild, average, and severe—were 18.38%, 27.09%, 26.12%, and 28.38%, respectively. The participants' responses in the questionnaires were subjected to an analysis of variance (ANOVAs) and the nonparametric test (Mann–Whitney) for parameters that were not normally distributed. However, the analysis did not exhibit any group differences in the age, $F(1, 88) = 2.664$, $p = 054$, $\eta 2 = 0.093$. Compared to all groups, severe participants have exhibited significantly higher SAD scores during the experiment: $F(1, 88) = 31.06$, $p = 0.001$, $\eta 2 = 0.53$.

5.2. Effective Connectivity in Different Frequency Bands

EC analysis was performed on artifact-free time series with smaller frequency rates to calculate the mean EEG activation in three DMN source-localized brain areas (PCC/Precuneus (PZ), LPC (CP5, CP6, P3, and P4), and mPFC/vmPFC (F3, F4, and FZ)). In the first experiment, the EC was calculated over the control, mild, average, and severe SAD groups and averaged within the subjects of each group. Then, the EC values were filtered into the different frequency rhythms (delta, theta, alpha, low beta, and high beta), as shown in Fig. 2.

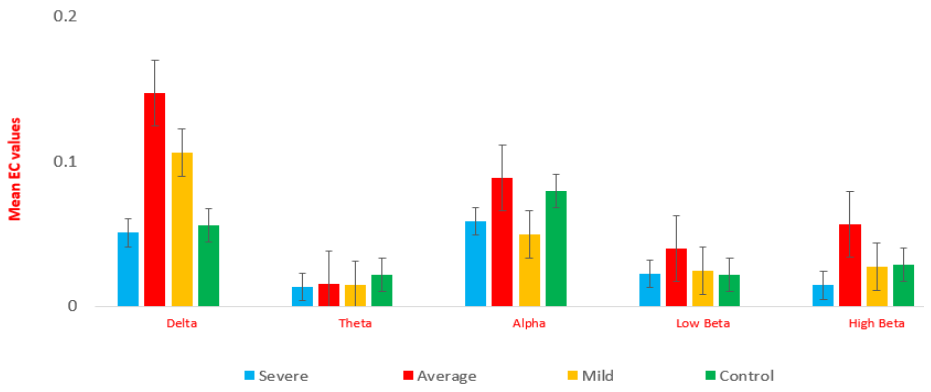

Fig.2. Average values of the EC across different frequency bands

The results in Fig. 2 indicate the significant difference among the four SAD groups (severe, average, mild, and control) in the delta and alpha bands: F (3, 252) = 3.937, p < 0.009, η 2 = 0.1 and F (3, 252) = 3.766, p < 0.01, η 2 = 0.1, respectively. In contrast to the alpha and delta bands, no significant differences in theta F (3, 252) = 1.98, p < 0.09, η2 = 0.51) and low beta (F (3, 252) = 0.410, p < 0.746, η 2 = 0.1) bands. In the delta band, post-hoc testing revealed significant 0.1466, SD = 0.3057) and mild (M = 0.1064, SD = 0.1586), while the control and severe groups exhibited less effective connections of (M = 0.0563, SD = 0.0512) and (M = 0.0514, SD = 0.1052), respectively were observed in the high beta (F (3, 252) = 1.571, p < 0.196, η2 = 0.1) and low beta (F (3, 252) = 0.410, p < 0.746, η 2 = 0.1) bands. This suggests that there were stronger connections among the DMN regions in the average and mild groups compared with the severe and control groups. The average and mild groups are found to show more functional control and strong attention compared to the severe group (Al-Ezzi et al., 2021), (Al-Ezzi et al., 2021). Moreover, in the alpha band, post-hoc testing revealed significant differences in the EC strengths between the groups; severe (M = 0.0587, SD = 0.0466), average (M = 0.0776, SD = 0.0707), control (M = 0.0797, SD = 0.0641), mild (M = 0.0501, SD = 0.0529). This indicates a stronger alpha connection in severe, average, and control groups more than mild group. Furthermore, the results indicated significant differences in the theta band between the severe and HC groups for F (3,252) = 2.389, p < 0.05, η 2 = 0.1, (M = 0.0141, SD = 0.0098), (M = 0.0216, SD = 0.0209), respectively. However, the results revealed no significant difference between the rest of the groups, F (3, 252) = 2.389, p <.069, η 2 = 0.1, average (M = 0.0163, SD = 0.0024), and mild (M = 0.0147, SD = 0.0024). As mentioned previously, the high beta and low beta did not exhibit any significant differences between any groups ((3, 252) = 1.571, p < 0.196, η 2 = 0.1), F (3, 252) = .410, p < .746, η 2 = 0.1). In the high beta band, the mean EC values were as follows: severe (M = 0.0242, SD = 0.0200), average (M = 0.0371, SD = 0.0515), mild (M = 0.278, SD = 0.034), and differences between the two different groups of average (M = control (M = 0.291, SD = 0.0356).

In the low beta band, the mean EC values were as follows: severe (M = 0.23, SD = 0.0172), average (M = 0.251, SD = 0.0286), mild (M = 0.254, SD = 0.0244), and control (M = 0.022, SD = q0.0178). The topographic mapping of averaged mean EC values at the various DMN regions during the resting-state are shown at different EEG bands in Fig. 3.

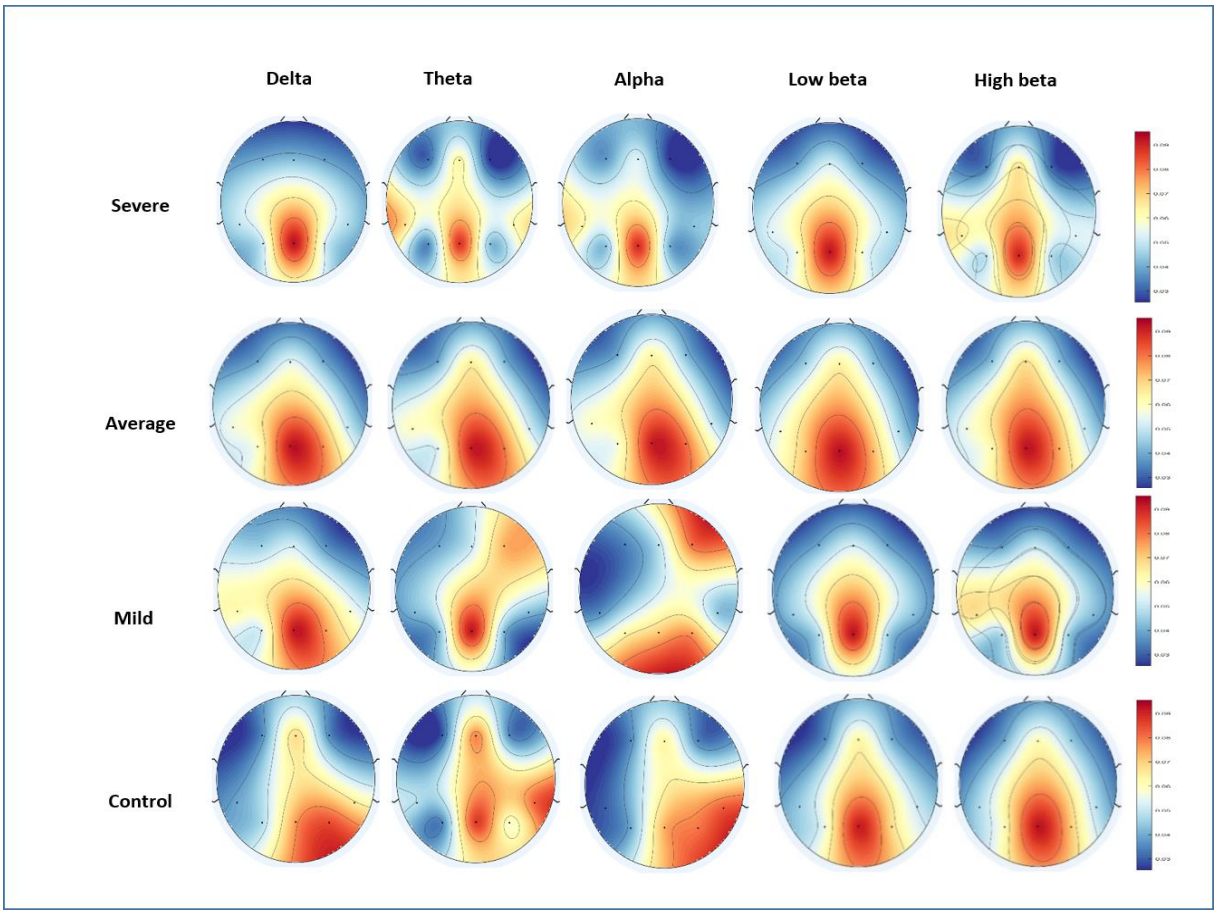

Fig.3. Topological maps of the mean total EC for all four SAD groups in the frequency bands. Red indicates a greater EC; blue indicates a smaller EC.

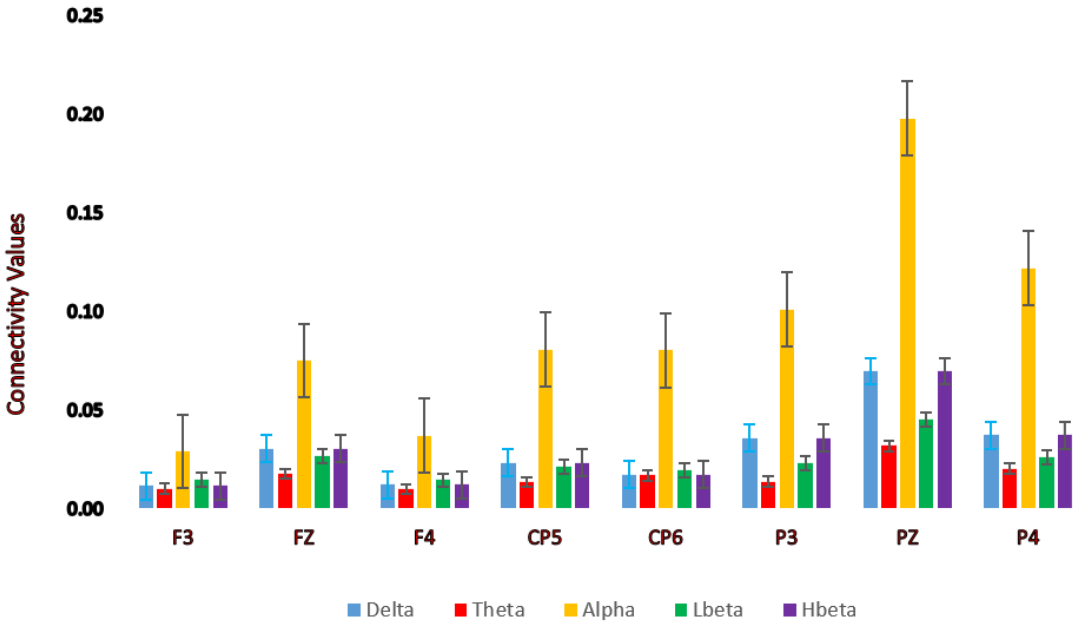

Fig.4. Relationship between the EC connectivity and the regional DMN areas.

Clearly, the precuneus region exhibited the strongest EC among the DMN regions. To address these differences statistically, Table 1 presents the ANOVA comparisons between EC values over the DMN regions. Fig. 4 presents the distribution of the EC over the DMN regions at the different EEG bands. The results indicated greater EC values in the alpha and delta frequency bands in DMN regions compared with the other frequency bands for all four groups. Among the DMN regions, the delta and alpha bands were higher in the LPC and precuneus than in the other DMN regions, in agreement with previous findings (Knyazev et al., 2004). Therefore, the PCC/precuneus is suggested to be a major source hub that contributes to the function and mechanism of cognitive exploration and emotional states of SAD. This fact might be helpful for the design of an effective evolutionary approach in social emotions to provide a conducive perception of the emotional environment in SAD. The ANOVA test in the ROI analysis revealed significantly greater EC values in the precuneus than in all other ROIs (Amodio et al., 2006). The reported findings are consistent with those for the DMN (Raichle et al., 2001). Moreover, the findings reveal that the precuneus is more active when individuals with SAD are in the DMN resting state, and it is implicated in a neural network of self-awareness, autobiographical tasks (Spreng, 2012) , cognitive interpretation and future planning (Northoff et al., 2006).

TABLE 1: ANOVA COMPARISONS BETWEEN EC VALUES, SAD GROUPS AND DMN REGIONS

Frequency Bands	Group	Mean	SD	F	*P* value	η 2
Delta	Control	0.105	0.016	3.937	0.009	0.1
	Mild	0.104	0.039			
	Moderate	0.105	0.041			
	Severe	0.121	0.055			
Theta	Control	0.133	0.130	1.98	0.09	0.051
	Mild	0.172	0.153			
	Moderate	0.157	0.092			
	Severe	0.220	0.102			
Alpha	Control	0.130	0.014	3.766	0.01	0.1
	Mild	0.109	0.041			
	Moderate	0.160	0.043			
	Severe	0.234	0.077			
Low Beta	Control	0.109	0.0149	1.571	0.196	0 .096
	Mild	0.110	0.045			
	Moderate	0.106	0.041			
	Severe	0.135	0.066			
High Beta	Control	0.109	0.016	0.410	0.746	0 .1
	Mild	0.110	0.039			
	Moderate	0.106	0.041			
	Severe	0.135	0.055			

Conclusion

This study was the first investigation of the DMN-EC network for SAD in different frequency bands. The use of directed EC estimates was suggested, and networks were identified via PDC analysis to evaluate the effect of SAD in DMN brain areas. Therefore, our findings indicated that individuals with SAD not only had abnormal alteration processing of certain socially anxious triggers but also exhibited stronger disturbance emotion processing in the basic nervous system pathway. The results reported herein are useful for the development of cognitive therapy models and the treatment of SAD. We reported a discriminatory deterioration or abnormality in the neural activity of the precuneus, mPFC, and LPC in severe SAD patients. It is believed that these regions with abnormal activations are biomarkers of SAD, representing the rudimentary pathophysiology and deficiency in the SAD groups. Overall, the subjective and behavioral findings indicate that EEG observations of the effects of SAD on emotional and cognitive processes in the DMN can serve as valuable biomarker indices for SAD diagnosis and treatment. Our analysis framework can be utilized in neuroscience research.

References

Al-Ezzi A., Kamel N., Faye I., and Gunaseli E. (2020), "Review of EEG, ERP, and Brain Connectivity Estimators as Predictive Biomarkers of Social Anxiety Disorder," Frontiers in Psychology, vol. 11. Frontiers Media S.A.

Al-Ezzi A., Kamel N., Faye I., and Gunaseli E. (2021), "Analysis of Default Mode Network in Social Anxiety Disorder: EEG Resting-State Effective Connectivity Study," Sensors 2021, Vol. 21, Page 4098, vol. 21, no. 12, p. 4098.

Al-Ezzi A., Yahya N., Kamel N., Faye I., Alsaih K., and Gunaseli E. (2021), "Severity Assessment of Social Anxiety Disorder Using Deep Learning Models on Brain Effective Connectivity," IEEE Access, vol. 9, pp. 86899–86913.

Amodio D. M. and Frith C. D. (2006), "Meeting of minds: The medial frontal cortex and social cognition," Nature Reviews Neuroscience, vol. 7, no. 4. Nat Rev Neurosci, pp. 268–277.

Andreescu C., Sheu L. K., Tudorascu D., Walker S., and Aizenstein H. (2014), "The ages of anxiety - Differences across the lifespan in the default mode network functional connectivity in generalized anxiety disorder," Int. J. Geriatr. Psychiatry, vol. 29, no. 7, pp. 704–712.

Baccalá L. A. and Sameshima K. (2001), "Partial directed coherence: A new concept in neural structure determination," Biol. Cybern., vol. 84, no. 6, pp. 463–474.

Bakhshayesh H., Fitzgibbon S. P., Janani A. S., Grummett T. S., and Pope K. J. (2019), "Detecting connectivity in EEG: A comparative study of data-driven effective connectivity measures," Comput. Biol. Med., p. 103329.
Beaty R. E., Seli P., and Schacter D. L. (2019), "Network neuroscience of creative cognition: mapping cognitive mechanisms and individual differences in the creative brain," Curr. Opin. Behav. Sci., vol. 27, pp. 22–30.

Blinowska K. J. (2011), "Review of the methods of determination of directed connectivity from multichannel data," Medical and Biological Engineering and Computing, vol. 49, no. 5. Springer, pp. 521–529.

Brigham K. and Kumar B. V. K. V. (2010), "Subject identification from Electroencephalogram (EEG) signals during imagined speech," in IEEE 4th International Conference on Biometrics: Theory, Applications and Systems, BTAS 2010.

Busby N., Halai A. D., Parker G. J. M., Coope D. J., and Ralph M. A. L. (2019), "Mapping whole brain connectivity changes: The potential impact of different surgical resection approaches for temporal lobe epilepsy," Cortex, vol. 113, pp. 1–14.

Chen A. C. and Etkin A. (2013), "Hippocampal network connectivity and activation differentiates post-traumatic stress disorder from generalized anxiety disorder," Neuropsychopharmacology, vol. 38, no. 10, pp. 1889–1898.

Delorme A. and Makeig S. (2004), "EEGLAB: an open sorce toolbox for analysis of single-trail EEG dynamics including independent component anlaysis," J. Neurosci. Methods, vol. 134, pp. 9–21.

Ding J. et al. (2011), "Disrupted functional connectivity in social anxiety disorder: A resting-state fMRI study," Magn. Reson. Imaging, vol. 29, no. 5, pp. 701–711.

Engel A. K., Fries P., and Singer W. (2001), "Dynamic predictions: oscillations and synchrony in top--down processing," Nat. Rev. Neurosci., vol. 2, no. 10, p. 704.

Fraga González G. et al. (2016), "Graph analysis of EEG resting state functional networks in dyslexic readers," Clin. Neurophysiol., vol. 127, no. 9, pp. 3165–3175.

Freitas-Ferrari M. C. et al. (2010), "Neuroimaging in social anxiety disorder: a systematic review of the literature," Prog. Neuro-Psychopharmacology Biol. Psychiatry, vol. 34, no. 4, pp. 565–580.

Grech R. et al. (2008), "Review on solving the inverse problem in EEG source analysis," Journal of NeuroEngineering and Rehabilitation, vol. 5, no. 1. BioMed Central, p. 25.

Greicius M. D., Supekar K., Menon V., and Dougherty R. F. (2009), "Resting-state functional connectivity reflects structural connectivity in the default mode network," Cereb. cortex, vol. 19, no. 1, pp. 72–78.

Hoehn Saric R. (1982), "Neurotransmitters in Anxiety," Arch. Gen. Psychiatry, vol. 39, no. 6, pp. 735–742.
Imperatori C. et al. (2014), "Aberrant EEG functional connectivity and EEG power spectra in resting state post-traumatic stress disorder: A sLORETA study," Biol. Psychol., vol. 102, no. 1, pp. 10–17.

Kessler R. C., Stang P., Wittchen H. U., Stein M., and Walters E. E. (1999), "Lifetime co-morbidities between social phobia and mood disorders in the US national comorbidity survey," Psychol. Med., vol. 29, no. 3, pp. 555–567.

Knyazev G. G., Savostyanov A. N., and Levin E. A. (2004), "Alpha oscillations as a correlate of trait anxiety," Int. J. Psychophysiol., vol. 53, no. 2, pp. 147–160.

Koyuncu A., İnce E., Ertekin E., and Tükel R. (2019), "Comorbidity in social anxiety disorder: Diagnostic and therapeutic challenges," Drugs in Context, vol. 8. Bioexcel Publishing LTD.

Lemyre A., Gauthier-Légaré A., and Bélanger R. E. (2019), "Shyness, social anxiety, social anxiety disorder, and substance use among normative adolescent populations: A systematic review," American Journal of Drug and Alcohol Abuse, vol. 45, no. 3. Taylor and Francis Ltd, pp. 230–247.

Liao W. et al. (2010), "Altered effective connectivity network of the amygdala in social anxiety disorder: a resting-state FMRI study," PLoS One, vol. 5, no. 12, p. e15238.

Liebowitz M. R., Gorman J. M., Fyer A. J., and Klein D. F. (1985), "Social Phobia: Review of a Neglected Anxiety Disorder," Arch. Gen. Psychiatry, vol. 42, no. 7, pp. 729–736.

Lin P. et al. (2017), "Dynamic Default Mode Network across Different Brain States," Sci. Rep., vol. 7, no. April, pp. 1–13.

Lopez Rincon A. and Shimoda S. (2016), "The inverse problem in electroencephalography using the bidomain model of electrical activity," J. Neurosci. Methods, vol. 274, pp. 94–105.

Northoff G., Heinzel A., de Greck M., Bermpohl F., Dobrowolny H., and Panksepp J. (2006), "Self-referential processing in our brain-A meta-analysis of imaging studies on the self," Neuroimage, vol. 31, no. 1, pp. 440–457.

Pascual-Marqui R. D. (1985), "Discrete, 3D distributed linear imaging methods of electric neuronal activity. Part 1: exact, zero error localization,"

Pascual-Marqui R. D. et al. (2011), "Assessing interactions in the brain with exact low-resolution electromagnetic tomography," Philos. Trans. R. Soc. A Math. Phys. Eng. Sci., vol. 369, no. 1952, pp. 3768–3784.

Pittig A., Arch J. J., Lam C. W. R., and Craske M. G. (2013), "Heart rate and heart rate variability in panic, social anxiety, obsessive--compulsive, and generalized anxiety disorders at baseline and in response to relaxation and hyperventilation," Int. J. Psychophysiol., vol. 87, no. 1, pp. 19–27.

Qiu C. et al. (2011), "Regional homogeneity changes in social anxiety disorder: A resting-state fMRI study," Psychiatry Res. - Neuroimaging, vol. 194, no. 1, pp. 47–53.

Raichle M. E., MacLeod A. M., Snyder A. Z., Powers W. J., Gusnard D. A. (2001), and Shulman G. L., "A default mode of brain function," Proc. Natl. Acad. Sci. U. S. A., vol. 98, no. 2, pp. 676–682.

Richards T. L. et al. (2015), "Contrasting brain patterns of writing-related DTI parameters, fMRI connectivity, and DTI--fMRI connectivity correlations in children with and without dysgraphia or dyslexia," NeuroImage Clin., vol. 8, pp. 408–421.

Sheline Y. I. et al. (2019), "The default mode network and self-referential processes in depression," Proc. Natl. Acad. Sci. U. S. A., vol. 106, no. 6, pp. 1942–1947.

Sladky R. et al. (2013), "Disrupted effective connectivity between the amygdala and orbitofrontal cortex in social anxiety disorder during emotion discrimination revealed by dynamic causal modeling for fMRI," Cereb. Cortex, vol. 25, no. 4, pp. 895–903.

Sokolov A. A., Zeidman P., Erb M., Ryvlin P., Pavlova M. A., and Friston K. J. (2019), "Linking structural and effective brain connectivity: Structurally informed parametric empirical Bayes (si-PEB)," Brain Struct. Funct., vol. 224, no. 1, pp. 205–217.

Spencer M. D. et al. (2012), "Failure to deactivate the default mode network indicates a possible endophenotype of autism," Mol. Autism, vol. 3, no. 1.

Spreng R. N. (2012), "The Fallacy of a 'Task-Negative' Network," Front. Psychol., vol. 3, no. MAY, p. 145.

Stein M. B. and Stein D. J. (2008), "Social anxiety disorder," The Lancet, vol. 371, no. 9618. Lancet, pp. 1115–1125.

Tao Y. et al. (2015), "The Structural Connectivity Pattern of the Default Mode Network and Its Association with Memory and Anxiety," Front. Neuroanat., vol. 9, no. November, pp. 1–10.

Valdes-Sosa P. A., Roebroeck A., Daunizeau J., and Friston K. (2011), "Effective connectivity: influence, causality and biophysical modeling," Neuroimage, vol. 58, no. 2, pp. 339–361.

Valdes-Sosa P. A., Roebroeck A., Daunizeau J., and Friston K. (2011), "Effective connectivity: Influence, causality and biophysical modeling," NeuroImage, vol. 58, no. 2. Academic Press, pp. 339–361.

Ventura J., Liberman R. P., Green M. F., Shaner A., and Mintz J. (1998), "Training and quality assurance with the structured clinical interview for DSM-IV (SCID-I/P)," Psychiatry Res., vol. 79, no. 2, pp. 163–173.

Von Dawans B., Trueg A., Kirschbaum C., Fischbacher U., and Heinrichs M. (2018), "Acute social and physical stress interact to influence social behavior: The role of social anxiety," PLoS One, vol. 13, no. 10, p. e0204665.

Wolpaw J. R., Birbaumer N., McFarland D. J., Pfurtscheller G., and Vaughan T. M. (2002), "Brain-computer interfaces for communication and control," Clinical Neurophysiology, vol. 113, no. 6. Elsevier, pp. 767–791.

Yu M. et al. (2016), "Different functional connectivity and network topology in behavioral variant of frontotemporal dementia and Alzheimer's disease: An EEG study," Neurobiol. Aging, vol. 42, pp. 150–162.